




Article

Recovery of Titanium and Aluminum from Secondary Waste Solutions via Ultrasonic Spray Pyrolysis

Srećko Stopić^{1,*}, Duško Kostić^{1,2} , Vladimir Damjanović³ , Mitar Perušić² , Radislav Filipović^{2,3}, Nenad Nikolić⁴ and Bernd Friedrich¹ 

¹ IME Process Metallurgy and Metal Recycling, RWTH Aachen University, 52056 Aachen, Germany; dkostic@metallurgie.rwth-aachen.de (D.K.); bfriedrich@metallurgie.rwth-aachen.de (B.F.)

² Faculty of Technology Zvornik, University of East Sarajevo, Karakaj 34A, 75400 Zvornik, Republic of Srpska, Bosnia and Herzegovina; mitar.perusic@tfzv.ues.rs.ba (M.P.); radislav.filipovic@birac.ba (R.F.)

³ Alumina d.o.o., Karakaj, 75400 Zvornik, Republic of Srpska, Bosnia and Herzegovina; vladimir.damjanovic@birac.ba

⁴ Institute for Multidisciplinary Research, University of Belgrade, Volgina 15, 11000 Belgrade, Serbia; nnikolic@imsi.bg.ac.rs

* Correspondence: sstopic@metallurgie.rwth-aachen.de; Tel.: +49-17678261674

Abstract

The synthesis of oxide nanopowders through ultrasonic spray pyrolysis (USP) represents a sustainable method for producing high-purity, spherical particles tailored for advanced material applications. Recent developments in USP synthesis leverage the continuous transport of aerosols from an ultrasonic generator to a high-temperature furnace, with nanopowders collected efficiently using an electrostatic precipitator. This study explored the use of USP for titanium oxysulfate and aluminum nitrate solutions derived from the aluminum industry, focusing on resource recovery and waste reduction. Titanium oxysulfate was synthesized by leaching slag, generated during the reduction of red mud, with sulfuric acid under oxidizing, high-pressure conditions. After purification, the titanium oxysulfate solution was processed using USP in a hydrogen reduction atmosphere to yield spherical titanium dioxide (TiO₂) nanopowders. The hydrogen atmosphere enabled precise control over the nanoparticles' morphology and crystallinity, enhancing their suitability for use in applications such as photocatalysis, pigments, and advanced coatings. In parallel, both synthetic and laboratory solutions of aluminum nitrate [Al(NO₃)₃] were prepared. The laboratory solution was prepared by leaching aluminum hydroxide oxide (AlOOH) with hydrochloric acid to form aluminum chloride (AlCl₃), followed by a conversion to aluminum nitrate through the addition of nitric acid. The resulting aluminum nitrate solution was subjected to USP, producing highly uniform, spherical alumina (Al₂O₃) nanopowders with a narrow size distribution. The resulting nanopowders, characterized by their controlled properties and potential applicability, represent an advancement in oxide powder synthesis and resource-efficient manufacturing techniques.

Keywords: hydrogen reduction; oxide nanopowders; ultrasonic spray pyrolysis; waste minimization



Academic Editor: Petros E. Tsakiridis

Received: 13 May 2025

Revised: 18 June 2025

Accepted: 19 June 2025

Published: 24 June 2025

Citation: Stopić, S.; Kostić, D.; Damjanović, V.; Perušić, M.; Filipović, R.; Nikolić, N.; Friedrich, B. Recovery of Titanium and Aluminum from Secondary Waste Solutions via Ultrasonic Spray Pyrolysis. *Metals* **2025**, *15*, 701. <https://doi.org/10.3390/met15070701>

Copyright: © 2025 by the authors. Licensee MDPI, Basel, Switzerland. This article is an open access article distributed under the terms and conditions of the Creative Commons Attribution (CC BY) license (<https://creativecommons.org/licenses/by/4.0/>).

1. Introduction

The ultrasonic spray pyrolysis (USP) technique is a droplet generation phenomenon induced by ultrasonic waves with several interesting properties, including its simplicity, cost-effectiveness, continuous operation, high deposition rate, and ability to deposit on

broad surface areas [1,2]. The size of the obtained droplets is less than 20 μm in average for a low in-flight speed. This can impede the removal of droplets from the gas phase due to their collision with the reactor walls and collisions between the droplets themselves and the consequent merging.

The spray pyrolysis technique has several advantages, including the higher stability of the obtained coatings as compared to coatings deposited in vacuum, the diversity of its solution precursors, its cost-effectiveness, and its ease of use.

The spray pyrolysis technique is an adaptable processing method for preparing single- and multi-layered films as dense or porous ceramic coatings and various material powders.

Ultrasonic atomization operates based on an electromechanical device vibrating at high frequencies. Only Newtonian fluids with low viscosities can be atomized when being passed over the vibrating surface, and the vibration causes the solution to be atomized into droplets.

As compared to the other techniques for depositing thin films, the spray pyrolysis technique has several advantages, including its open-atmosphere process, its open reaction chamber, its adjustability during deposition, and the ability to observe the deposition procedure [3].

Due to the easily controllable morphologies of the powders obtained using the USP method as well as the availability of its inexpensive precursors, it is a versatile and powerful tool for synthesizing particles of controlled as well as uniform particle sizes. This technique has great potential for synthesizing nanoscale metallic and oxidic particles [4–6]. Zhao et al. performed the synthesis of core–shell particles using the ultrasonic spray pyrolysis synthesis of Ag/TiO₂ Nanocomposite Photocatalysts for simultaneous H₂ production and CO₂ reduction [7]. Because of its excellent properties, titanium oxide was used as a carrier for catalytic active silver particles.

In the USP method, the starting solution precursor is atomized to form an aerosol [8–11]. Droplets of the aerosol are carried by a carrier gas, usually a reducing gas, into a hot chamber, where the droplets are dried, contracted, precipitated, thermolized, and sintered, and spherical particles will be formed. Very short residence times, typically of a few seconds, are usually sufficient in order to guarantee the formation of spherical nanoparticles [12–14].

The size of the obtained nanoparticles is related to the droplet diameter and the initial concentration of the precursor solution [15]. Increasing the ultrasonic frequency reduces the droplet diameter of the produced aerosol and also increases the ratio of smaller nanoparticles in the final product. The formation of droplets by ultrasound was first described by Wood and Loomis in 1927. Lang [16], in 1962, and Peskin and Raco [17], in 1963, formulated an equation to describe the connection between the ultrasonic frequency and the mean droplet diameter. A theoretical equation for the prediction of the sizes of the obtained nanoparticles was formulated in previous work, combining Kelvin's equation and an equation based on the capillary theory.

$$D_{mat} = 0.34 \left(\frac{8\pi \sigma C_{sol} M_{mat}}{\rho_{sol} f M_{sol} \rho_{mat}} \right)^{\frac{1}{3}} \quad (1)$$

D_{mat} is the final particle diameter; C_{sol} , ρ_{sol} , and M_{sol} are the solute concentration, density, and molar mass; M_{mat} and ρ_{mat} are the molar mass and density of the desired material; σ is the surface tension; and f is the frequency of the ultrasonic atomizer.

Stopić et al. [18] synthesized nanosized TiO₂ particles from C₁₆H₃₆O₄Ti using ultrasonic spray pyrolysis (USP) in single- and multi-step processes with horizontal and vertical reactors. Spherical submicron TiO₂ core–RuO₂ shell particles were obtained via multi-step USP using two ultrasonic atomizers (0.8 MHz and 2.5 MHz) fed with separate RuCl₄ and C₁₆H₃₆O₄Ti solutions at 850 °C in oxidizing conditions. Particle characterization was

performed using XRD, SEM, and TEM, with the core–shell structure confirmed through a comparison with a hard sphere model. It was shown that the aerosol mixing of Ru and TiO₂ streams significantly affected core–shell formation.

In a follow-up study [19], RuO₂/TiO₂ particles synthesized by USP from a mixed solution were deposited on titanium substrates in a second reactor under a high-voltage electrostatic field at 500 °C. The coatings' electrochemical behavior was studied, establishing structure–activity/stability correlations for the TiO₂@RuO₂ microspheres.

To avoid the use of carbon-based precursors [20,21], Kostić et al. [22] investigated the thermal decomposition of titanium oxysulfate via USP between 700 and 1000 °C. The effects of the solution concentration and H₂/Ar flow rates were examined. The resulting powders exhibited a spherical morphology and varied in size based on the process conditions. However, wet powder collection led to material loss, prompting the current study's use of electrostatic precipitation for improved recovery.

Other studies have confirmed USP's efficacy in producing oxide nanoparticles like alumina and ZnO [23–25]. Janacković et al. [26] synthesized spherical alumina particles via USP from 0.5 M aqueous solutions of aluminum nitrate and chloride at 800–1000 °C. Yet, these studies focused on pure precursors and did not implement advanced powder collection.

This study presents a novel application of USP for synthesizing TiO₂ and Al₂O₃ nanopowders from industrial waste-derived precursors such as red mud (bauxite residue), a byproduct of the Bayer process [27,28]. With ~180 million tons generated annually and over 4 billion tons accumulated [29,30], red mud poses a serious environmental challenge. By incorporating electrostatic precipitation, this work improved the collection efficiency and purity while promoting resource recovery and environmental sustainability.

2. Materials and Methods

Ultrasonic spray pyrolysis (USP) was employed for the synthesis of aluminum oxide (Al₂O₃) and titanium dioxide (TiO₂) nanopowders, with hydrogen reduction applied exclusively in the production of the titanium-based powders. For aluminum oxide synthesis, aluminum nitrate was prepared by dissolving aluminum hydroxide oxide (AlOOH) in hydrochloric acid to form aluminum chloride, followed by the addition of nitric acid to convert it into aluminum nitrate. In contrast, titanium oxysulfate was used as the precursor for TiO₂ synthesis under a hydrogen reduction atmosphere. This study introduces the novel application of titanium oxysulfate (TiOSO₄) and aluminum nitrate (Al(NO₃)₃) solutions as precursors for the production of nanosized TiO₂ and Al₂O₃ powders, addressing a significant gap in the literature. Both precursors, each with a 1 M molar concentration, were processed using an ultrasonic generator (PRIZNANO, Kragujevac, Serbia) to produce aerosols, highlighting the scalability and versatility of the USP method for oxide nanopowder synthesis. This furnace had 4 different heaters with a liquid tank with a pump for the continuous transport of the produced aerosols, as shown at Figure 1.

The temperature in the furnace was controlled and regulated during the experimental work. The reaction tube was made from stainless steel, and a ceramic tube was used for the second titanium dioxide nanopowder experiments. Both tubes had a diameter of 100 mm. The level of liquid fluid was regulated using a special sensor. The frequency of the ultrasound was 1.7 MHz. The production of the aerosols was 1 L/h. The transport of the produced aerosols was performed using air. The collection of the powder was performed using one electrostatic precipitator (voltage: 7–12 KV), as shown in Figure 2.

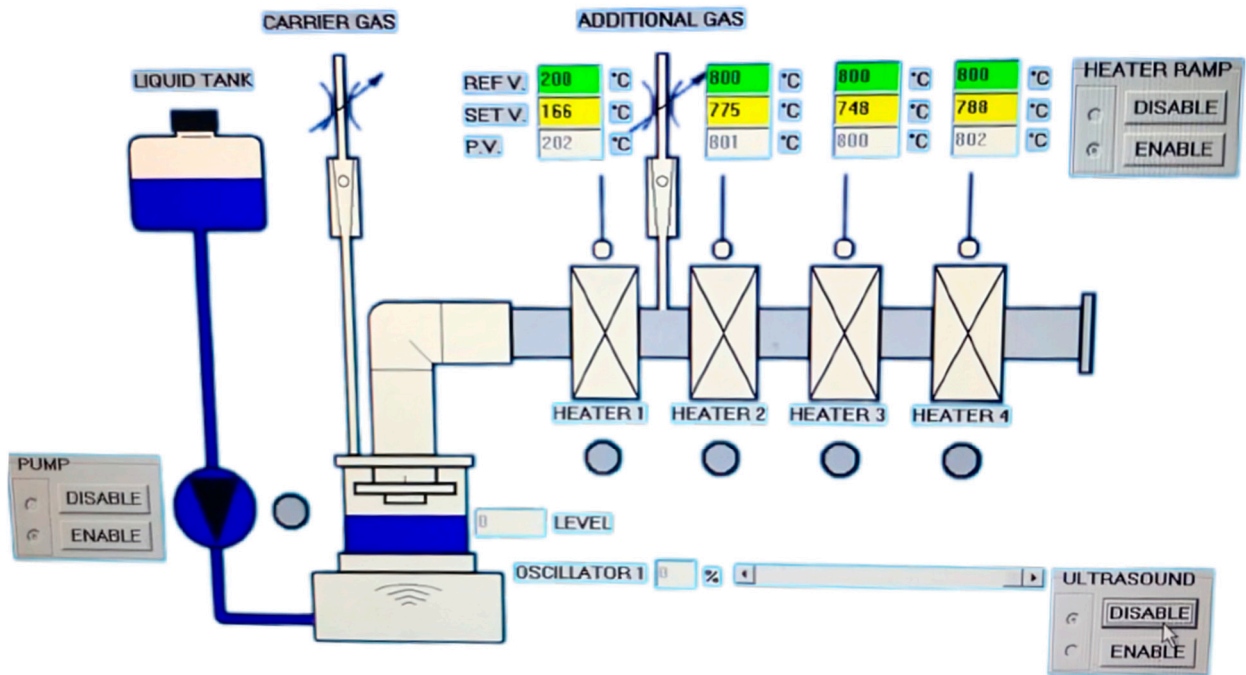


Figure 1. Scheme showing continuous transport of precursor from liquid tank and transport of aerosols to furnace with 4 heating zones.



Figure 2. Experimental setup for USP.

This image shows an advanced setup for ultrasonic spray pyrolysis (USP), highlighting its essential components for nanoparticle synthesis. On the left, the ultrasonic generator was used to atomize precursor solutions into a fine aerosol using ultrasonic waves. This step ensured the production of uniform droplets, which were then transported into the central unit, a high-temperature tubular furnace. The tubular furnace served as the reaction zone where the aerosol underwent thermal decomposition in a controlled environment, resulting in the formation of oxide powders. The furnace allowed for precise adjustments of the temperature and atmosphere, such as the reducing or inert gases, to achieve the desired material properties. On the right, the electrostatic precipitator efficiently captured the synthesized nanopowders. Employing an electrostatic field ensured the collection of the fine particles produced during pyrolysis, minimizing the material loss and ensuring environmental safety. The maximal temperature in the electrostatic precipitator was 200 °C in order to prevent condensation in the system, enabling the production of dried powder.

This integrated setup produced by PRIZMA, Kragujevac, Serbia, demonstrates the efficiency and precision of USP as a scalable method for producing high-purity oxide nanopowders like titanium dioxide (TiO₂) and aluminum oxide (Al₂O₃).

All the experiments were conducted using a PRIZNano generator. Various methods were used for sample characterization, which included XRD analysis, EDX analysis, particle size distribution measurements, and SEM analysis. SEM analysis was performed using the JSM 7000F by JEOL (manufactured in 2006, JEOL Ltd., Tokyo, Japan) coupled with EDX analysis using the Octane Plus-A by Ametek-EDAX (manufactured in 2015, AMETEK Inc., Berwyn, PA, USA), with the equipment operated using Genesis V 6.53 software by Ametek-EDAX. These analyses revealed the irregular structure of the precursor, as depicted in Figure 2. The XRD analysis of the obtained powders was carried out on a Bruker D8 Advance equipped with a LynxEye detector (Bruker AXS, Karlsruhe, Germany). The X-ray diffraction patterns were obtained using a Bruker-AXS D4 Endeavor diffractometer (Bruker AXS, Karlsruhe, Germany) in a Bragg–Brentano geometry. The system featured a copper tube and a primary nickel filter providing Cu K α 1,2 radiation ($\lambda = 1.54187 \text{ \AA}$). HighScore software, version 5.0, in conjunction with the COD database, was used to analyze the diffraction data.

3. Results

3.1. The Synthesis of the Aluminum Oxide Nanopowder

The experimental preparation of alumina powders from aqueous solutions of aluminum nitrate was carried out at a temperature of 1000 °C in a compressed air atmosphere, with a solution flow rate of 5 L/min. Two solutions were prepared; one was synthetic, prepared from pure aluminum nitrate, and the second was a laboratory solution obtained by dissolving a purified precursor in hydrochloric acid, followed by conversion to an aluminum nitrate solution using nitric acid. The ICP analysis of those two solutions is present in Table 1.

Table 1. ICP analysis of synthetic and laboratory solutions.

Solution	Al ₂ O ₃ , g/L	CaO, ppm	MgO, ppm	Fe ₂ O ₃ , ppm	Na ₂ O, ppm	PbO, ppm	ZnO, ppm	SiO ₂ , ppm
Laboratory	98.86	3.10	2.67	8.87	5.20	1.52	4.88	2.56
Synthetic	104.4	0.56	0.00	0.00	0.00	0.50	0.00	1.28

This table compares the impurity levels in two Al(NO₃)₃ solutions: one produced using the Bayer process (laboratory AlOOH) and the other from a pure chemical source (synthetic Al(NO₃)₃). The laboratory Al(NO₃)₃ contained more impurities due to its production using the Bayer process, which introduced elements like Fe₂O₃, Na₂O, and SiO₂ from bauxite. In contrast, the synthetic Al(NO₃)₃ had fewer impurities, being made from pure Al(NO₃)₃, and lacked Fe₂O₃ and Na₂O. The laboratory solutions contained Na₂O from the NaOH used in the Bayer process and Fe₂O₃ due to bauxite's iron content.

The obtained powders are shown in Figure 3.

The SEM images provided depict Al₂O₃ (alumina) nanoparticles synthesized through the ultrasonic spray pyrolysis of aluminum nitrate produced using (a) synthetic and (b) laboratory solutions. The particles exhibit a generally spherical morphology, indicating successful particle formation during the spray pyrolysis process. The uniform spherical shape is characteristic of the rapid droplet drying and subsequent solidification that occur in ultrasonic spray pyrolysis, in which the surface tension promotes spherical shapes.

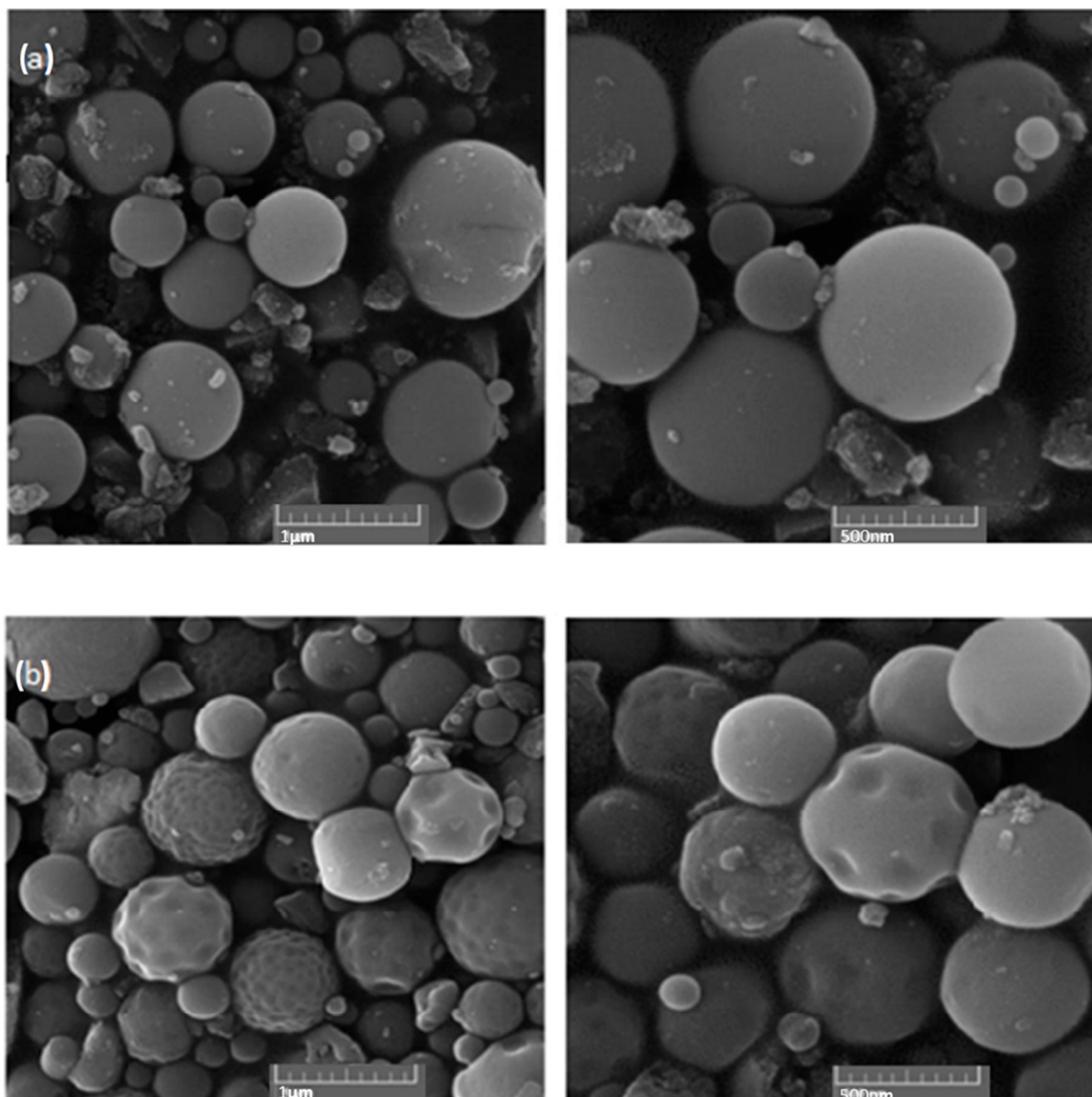


Figure 3. SEM analysis of aluminum oxide nanopowder obtained from (a) synthetic solution and (b) laboratory solution.

The size distribution appears relatively uniform, although a closer inspection reveals slight variations in the particle sizes. The scale bars indicate that most particles were within the sub-micrometer range, with some smaller nanoparticles visible as well. The higher-magnification image provides evidence of the surface texture of and minor structural irregularities in some particles in the nanopowder prepared from the laboratory solution, possibly due to rapid evaporation or precursor concentration effects during synthesis or from impurities, which were present slightly more in the laboratory solution.

The absence of significant agglomeration suggests effective control over the process parameters, such as the temperature, concentration, and residence time, during ultrasonic spray pyrolysis. The distinct separation of the particles further supports the high purity and stable dispersion of the precursor solution.

Figure 4 presents the EDS analysis of the nanopowder obtained from the (a) laboratory and (b) synthetic solutions. In both cases, peaks for aluminum (Al) and oxygen (O) are evident, confirming the presence of the Al_2O_3 nanopowder.

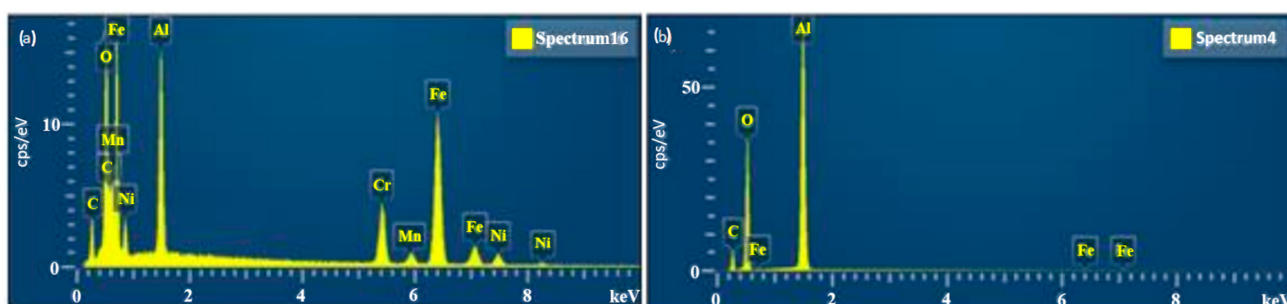


Figure 4. EDS analysis of the nanopowder obtained from the (a) laboratory and (b) synthetic solutions.

In panel (a) (laboratory solution), significant amounts of impurities such as Fe, Ni, Cr, Mn, and C can be observed. These impurities could have originated from several sources: the laboratory solution was obtained through digestion with HCl, which may have been present in the form of chloride ions. These ions could have caused corrosion in the furnace tube, which was made of stainless steel, during the ultrasonic spray pyrolysis (USP) process. Carbon (C) contamination may also have occurred due to the process itself. In Table 2, the composition of the stainless steel tube in the USP tubular furnace is shown.

Table 2. Chemical composition of stainless steel tube in USP tubular furnace.

Alloy Composition	C	Cr	Mn	Ni	P	Si
%	0.023	24.15	1.85	20.37	0.021	1.75

For the (b) synthetic solution, the EDS spectrum primarily shows peaks for Al and O, with small amounts of Fe and C. The presence of Fe and C was likely due to minimal equipment contamination during the synthesis process.

XRD analysis also confirmed the EDS results.

Figure 5 shows the XRD analysis for nanopowders obtained from the (a) laboratory and (b) synthetic solutions.

For the (a) laboratory solution, the XRD pattern primarily corresponded to a single phase, which was the most intense and resembled an Al-Fe-Si compound with a composition of $\text{Al}_{0.7}\text{Fe}_3\text{Si}_{0.3}$. This phase had the best match with the experimental data. It is suggested that the presence of iron (Fe) came from the corrosion of the stainless steel furnace tube during synthesis. The silicon (Si) could be a result of contamination from materials like glass or quartz used in the equipment.

For the (b) synthetic solution, the XRD showed peaks corresponding to different phases of Al_2O_3 , specifically gamma- Al_2O_3 modifications. These phases were similar, but there was no match with alpha- Al_2O_3 (corundum), which would be expected for pure alumina. Additionally, there were no signs of elemental aluminum or AlOOH . The gamma phase observed was of very low crystallinity, as indicated by the broad peaks in the XRD.

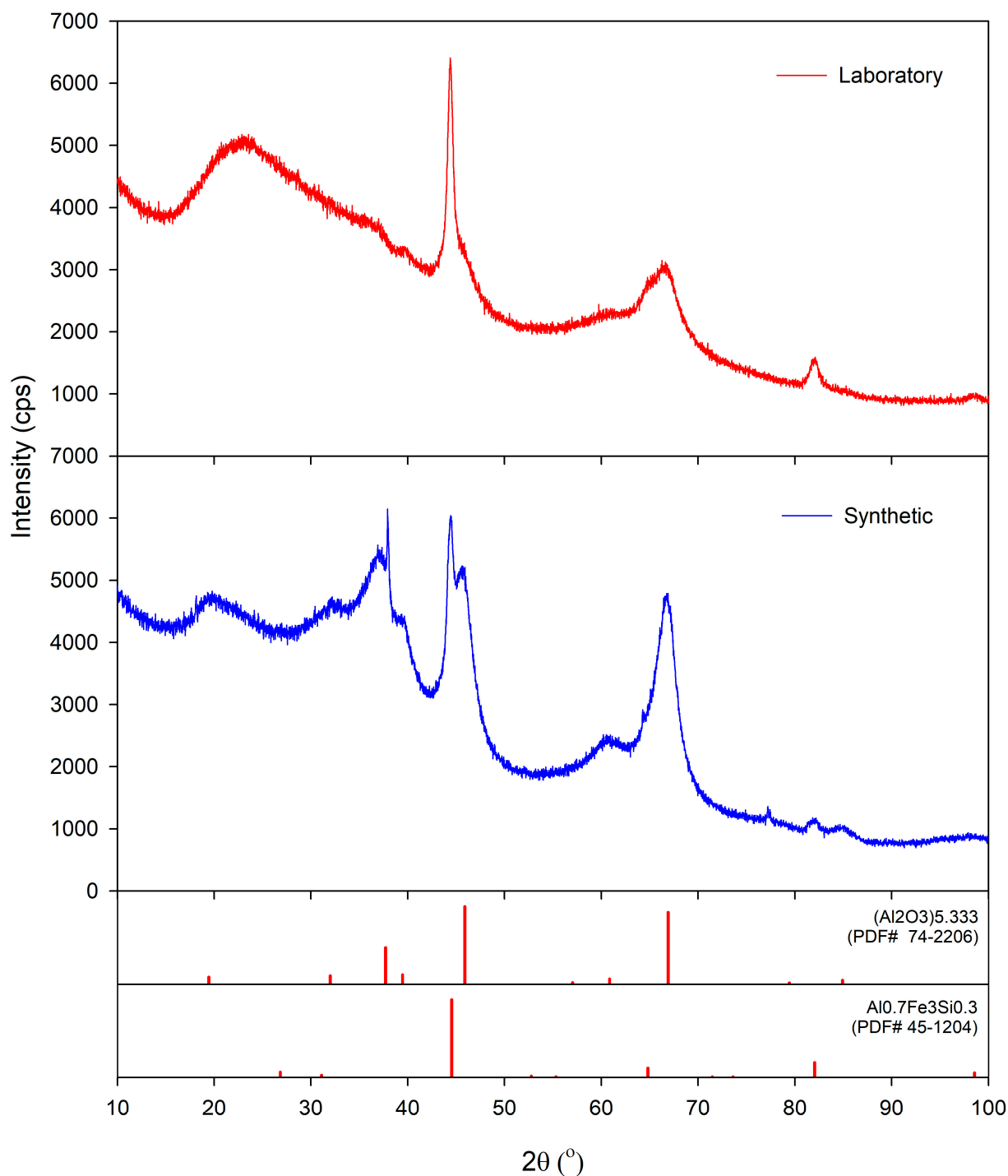


Figure 5. XRD analysis of nanopowder obtained from laboratory and synthetic solutions.

3.2. Synthesis of Titanium Dioxide Nanopowder

The experimental preparation of titanium powders from aqueous solutions of titanium oxysulfate was carried out the same as for the aluminum oxide at a temperature of 1000 °C in a compressed air atmosphere, with a solution flow rate of 5 L/min (a), and also at 1300 °C in a ceramic tube due to the high temperature. The solution used was obtained from red mud by purifying the solution obtained from the leaching process of red mud. The hydrogen reduction of titanium oxysulfate, combined with ultrasonic spray pyrolysis, led to the formation of spherical TiO₂ particles. The process appeared to be stable, as evidenced by the uniform particle size distribution, as shown in Figure 5. The first two experiments were performed in oxygen and inert atmospheres, and it was concluded that the transfor-

mation of titanium oxysulfate into titanium dioxide using the USP method is very slow or impossible without hydrogen.

The SEM image (Figure 6) shows that spherical particles formed through the ultrasonic spray pyrolysis process. The particles appeared uniform in shape, with a size range at the micrometer scale, approximately 0.5–1 μm for (a) and less than 1 μm at the nanoscale for (b). Some smaller particles were attached to the larger ones, indicating possible agglomeration during or after formation. This spherical morphology is typical for spray pyrolysis, which involves rapid solvent evaporation and solute precipitation during droplet decomposition.

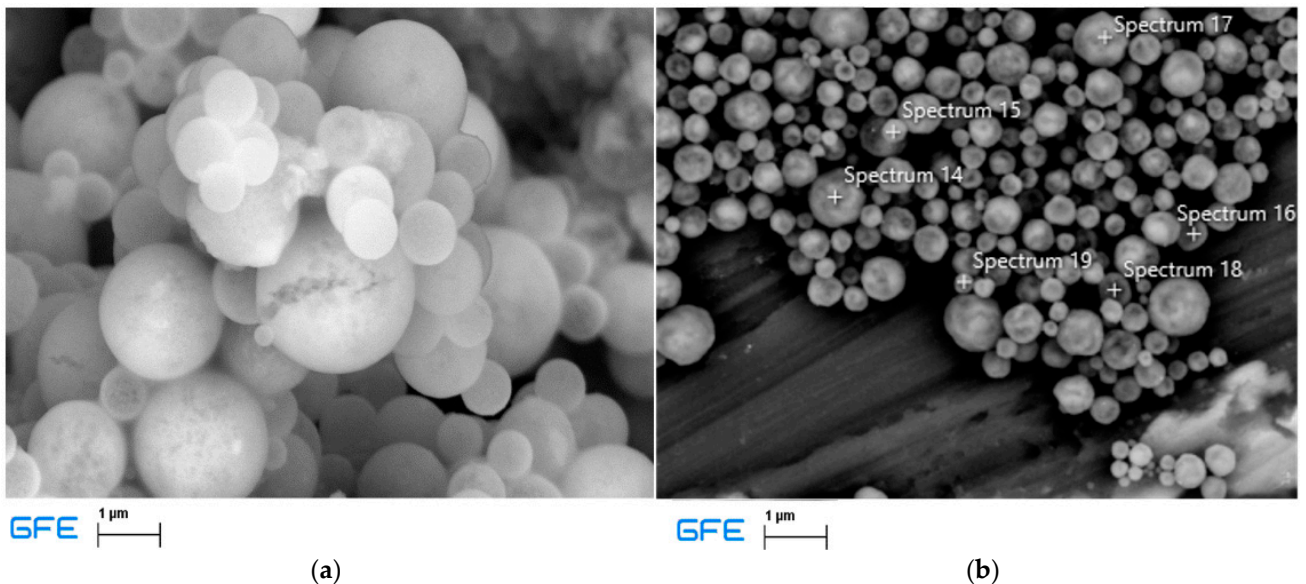


Figure 6. SEM analysis of titanium oxide nanopowder prepared at (a) 1000 $^{\circ}\text{C}$ and (b) 1300 $^{\circ}\text{C}$.

The EDS spectrum (Figure 7) reveals that the sample was primarily composed of oxygen and titanium for both samples, with quantified amounts of approximately 62 wt% oxygen and 38 wt% titanium for (a) and 40.8 wt% oxygen and 58.8 wt% titanium for (b). This composition aligns closely with that of titanium dioxide (TiO_2), suggesting that the material was likely a reduced or slightly oxygen-deficient form of TiO_2 . The O:Ti ratio (~ 1.63) was slightly below the ideal stoichiometry for TiO_2 , which may have resulted from the hydrogen reduction step, potentially creating oxygen vacancies in the structure. The absence of sulfur in the EDS spectrum indicates that sulfur species were successfully removed during the reduction process. Aluminum and copper peaks can be attributed to the carrier of the sample.

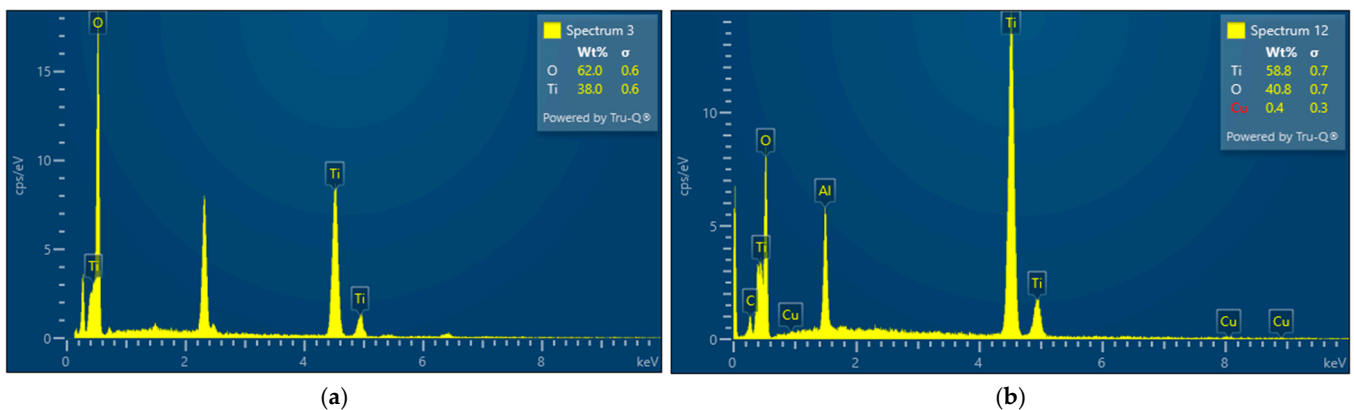


Figure 7. EDS analysis of TiO_2 nanopowder obtained at (a) 1000 $^{\circ}\text{C}$ and (b) 1300 $^{\circ}\text{C}$.

The provided XRD pattern (Figure 8) corresponds to the crystalline phases present in the sample. Based on the Rietveld refinement results, the sample was composed of only one phase, which was rutile, for (a) and anatase and rutile for (b) (the anatase phase accounted for 67.9% of the composition, while the rutile phase made up 32.1%). This composition of titanium dioxide (TiO_2) suggests that the temperature influenced the crystalline form of material.

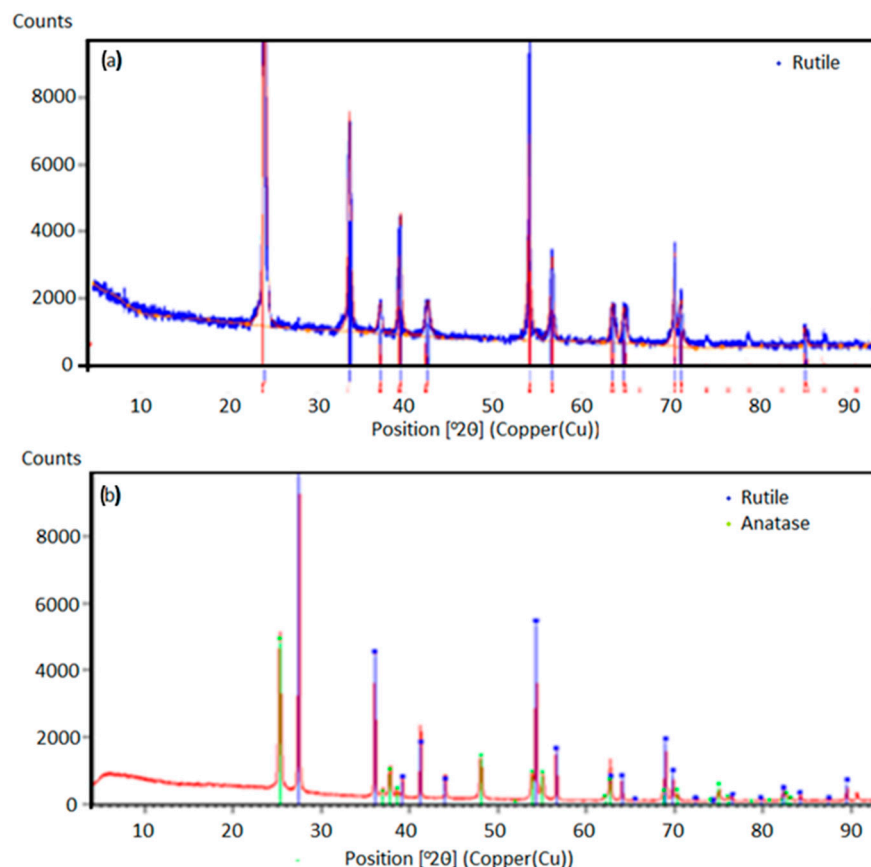


Figure 8. XRD analysis of titanium dioxide nanopowder produced at (a) 1000 °C and (b) 1300 °C.

The anatase phase was identified by its characteristic peaks at lower diffraction angles, which aligned with the reference data. Similarly, the rutile phase is distinguished by its sharper peaks at slightly higher angles. The presence of both phases can significantly influence the material's properties. Our results clearly show that higher temperatures favors the development of a rutile phase while lower temperatures favor the development of an anatase phase.

4. Conclusions

This study demonstrates the successful synthesis of aluminum oxide (Al_2O_3) and titanium dioxide (TiO_2) nanopowders via ultrasonic spray pyrolysis (USP), utilizing novel precursors derived from industrial byproducts. The experimental results highlight the effectiveness of USP in producing high-purity, spherical nanoparticles with a controlled morphology and uniform size distribution.

For Al_2O_3 synthesis, both laboratory and synthetic aluminum nitrate solutions were used as precursors. The laboratory solution, derived from AlOOH through the Bayer process, showed a higher presence of impurities, such as Fe, Ni, Cr, Mn, and C, which likely originated from the corrosion of the stainless steel equipment and contamination from the HCl digestion process. In contrast, the use of the synthetic aluminum nitrate

solution resulted in the production of Al₂O₃ nanoparticles with fewer impurities, primarily consisting of Al and O with small amounts of Fe and C. The EDS and XRD analyses confirmed the successful formation of alumina nanoparticles, with the laboratory solution yielding a phase likely related to an Al-Fe-Si compound, while the synthetic solution produced gamma-Al₂O₃ with low crystallinity, as indicated by the broad peaks in the XRD pattern.

The TiO₂ synthesis utilized titanium oxysulfate derived from leached titanium from reduced red mud, producing spherical TiO₂ particles. XRD analysis revealed a biphasic structure of anatase and rutile for the sample prepared at a lower temperature, while only the rutile phase was present at a higher temperature, indicating that the temperature can control phase formation and also the particle size.

The integration of electrostatic precipitators for efficient nanopowder collection further enhances the scalability and environmental sustainability of the USP process. This work highlights the importance of precursor choice and process control in achieving the production of high-quality materials. It underscores the potential of ultrasonic spray pyrolysis as a highly effective and resource-efficient method for producing oxide nanopowders from both synthetic and laboratory-derived precursors, offering new opportunities for sustainable manufacturing in the materials science industry.

Author Contributions: Conceptualization, S.S., R.F. and B.F.; methodology, S.S., D.K., M.P. and R.F.; software, V.D. and N.N.; validation, S.S. and V.D., formal analysis, D.K. and V.D.; investigation, D.K., R.F. and N.N.; resources, M.P., N.N. and B.F.; data curation, V.D. and M.P.; writing—original draft preparation, S.S., D.K. and V.D.; writing—review and editing, N.N.; visualization, M.P.; supervision, M.P., R.F. and B.F.; project administration, S.S., R.F. and B.F.; funding acquisition, B.F. All authors have read and agreed to the published version of the manuscript.

Funding: This research was funded by the European Commission, grant number 101135077 (EURO-TITAN).

Data Availability Statement: The original contributions presented in this study are included in the article. Further inquiries can be directed to the corresponding author.

Conflicts of Interest: Authors Vladimir Damjanović and Radislav Filipović were employed by Alumina d.o.o. The remaining authors declare that the research was conducted in the absence of any commercial or financial relationships that could be construed as a potential conflict of interest.

References

1. Majeric, P.; Rudolf, R. Advances in Ultrasonic Spray Pyrolysis Processing of Noble Metal Nanoparticles—Review. *Materials* **2020**, *13*, 3485. [[CrossRef](#)] [[PubMed](#)]
2. Rahemi Ardekani, S.; Sabour Rouh Aghdam, A.; Nazari, M.; Bayat, A.; Yazdani, E.; Saievar-Iranizad, E. A Comprehensive Review on Ultrasonic Spray Pyrolysis Technique: Mechanism, Main Parameters and Applications in Condensed Matter. *J. Anal. Appl. Pyrolysis* **2019**, *141*, 104631. [[CrossRef](#)]
3. Tsai, S.C.; Song, Y.L.; Tsai, C.S.; Yang, C.C.; Chiu, W.Y.; Lin, H.M. Ultrasonic Spray Pyrolysis for Nanoparticles Synthesis. *J. Mater. Sci.* **2004**, *39*, 3647–3657. [[CrossRef](#)]
4. Tiyyagura, H.R.; Majerič, P.; Anžel, I.; Rudolf, R. Low-Cost Synthesis of AuNPs through Ultrasonic Spray Pyrolysis. *Mater. Res. Express* **2020**, *7*, 055017. [[CrossRef](#)]
5. Mädler, L. Liquid-Fed Aerosol Reactors for One-Step Synthesis of Nano-Structured Particles. *KONA Powder Part. J.* **2004**, *22*, 107–120. [[CrossRef](#)]
6. Emil, E.; Alkan, G.; Gurmen, S.; Rudolf, R.; Jenko, D.; Friedrich, B. Tuning the Morphology of ZnO Nanostructures with the Ultrasonic Spray Pyrolysis Process. *Metals* **2018**, *8*, 569. [[CrossRef](#)]
7. Zhao, C.; Krall, A.; Zhao, H.; Zhang, Q.; Li, Y. Ultrasonic Spray Pyrolysis Synthesis of Ag/TiO₂ Nanocomposite Photocatalysts for Simultaneous H₂ Production and CO₂ Reduction. *Int. J. Hydrogen Energy* **2012**, *37*, 9967–9976. [[CrossRef](#)]
8. Milošević, O.; Jordovic, B.; Uskokovic, D. Preparation of Fine Spherical ZnO Powders by an Ultrasonic Spray Pyrolysis Method. *Mater. Lett.* **1994**, *19*, 165–170. [[CrossRef](#)]

9. Choi, W.J.; Kim, J.H.; Lee, H.; Park, C.W.; Lee, Y.I.; Byun, J. Hydrogen Reduction Behavior of W/Y₂O₃ Powder Synthesized by Ultrasonic Spray Pyrolysis. *Int. J. Refract. Met. Hard Mater.* **2021**, *95*, 105450. [[CrossRef](#)]
10. Ebin, B.; Gurmen, S. Synthesis and Characterization of Nickel Particles by Hydrogen Reduction Assisted Ultrasonic Spray Pyrolysis(USP-HR) Method. *KONA Powder Part. J.* **2011**, *29*, 134–140. [[CrossRef](#)]
11. Shatrova, N.; Yudin, A.; Levina, V.; Dzidziguri, E.; Kuznetsov, D.; Perov, N.; Issi, J.P. Elaboration, Characterization and Magnetic Properties of Cobalt Nanoparticles Synthesized by Ultrasonic Spray Pyrolysis Followed by Hydrogen Reduction. *Mater. Res. Bull.* **2017**, *86*, 80–87. [[CrossRef](#)]
12. Li, M.; Zhao, L.; Guo, L. Preparation and Photoelectrochemical Study of BiVO₄ Thin Films Deposited by Ultrasonic Spray Pyrolysis. *Int. J. Hydrogen Energy* **2010**, *35*, 7127–7133. [[CrossRef](#)]
13. Küçükelyas, B.; Safaltın, S.; Sam, E.D.; Gurmen, S. Synthesis, Structural and Magnetic Characterization of Spherical High Entropy Alloy CoCuFeNi Particles by Hydrogen Reduction Assisted Ultrasonic Spray Pyrolysis. *Int. J. Mater. Res.* **2022**, *113*, 306–315. [[CrossRef](#)]
14. Koo, Y.; Oh, S.; Im, K.; Kim, J. Ultrasonic Spray Pyrolysis Synthesis of Nano-Cluster Ruthenium on Molybdenum Dioxide for Hydrogen Evolution Reaction. *Appl. Surf. Sci.* **2023**, *611*, 155774. [[CrossRef](#)]
15. Rajan, R.; Pandit, A. Correlation to predict Droplet Size in Ultrasonic Atomisation. *Ultrasonics* **2001**, *39*, 235–255. [[CrossRef](#)]
16. Lang, R. Ultrasonic atomization of liquids. *J. Acoust. Soc. Am.* **1962**, *34*, 6–8. [[CrossRef](#)]
17. Peskin, R.L.; Raco, R.J. Ultrasonic Atomization of Liquids. *J. Acoust. Soc. Am.* **1963**, *35*, 1378–1381. [[CrossRef](#)]
18. Stopic, S.; Schroeder, M.; Weirich, T.; Friedrich, B. Synthesis of TiO₂ Core/RuO₂ Shell Particles using Multistep Ultrasonic Spray Pyrolysis. *Mater. Res. Bull.* **2013**, *48*, 3633–3635. [[CrossRef](#)]
19. Košević, M.; Stopic, S.; Bulan, A.; Kintrup, J.; Weber, R.; Stevanović, J.; Panic, V.; Friedrich, B. A continuous process for the ultrasonic spray pyrolysis synthesis of RuO₂-TiO₂ particles and their application as an active coating of activated titanium anode. *Adv. Powder Technol.* **2017**, *28*, 43–49. [[CrossRef](#)]
20. Ahonen, P.; Kauppinen, E.; Joubert, J.; Deschanvres, J.; Van Tendeloo, G. Preparation of Nanocrystalline Titania Powder via Aerosol Pyrolysis of Titanium tetrabutoxide. *J. Mater. Res.* **1999**, *14*, 3938–3948. [[CrossRef](#)]
21. Messing, G.; Zhang, S.; Jayanthi, G. Ceramic powder synthesis by spray pyrolysis. *J. Am. Ceram. Soc.* **1993**, *76*, 2707–2726. [[CrossRef](#)]
22. Kostic, D.; Stopic, S.; Keutmann, M.; Emil-Kaya, E.; Volkov-Husovic, T.; Perušić, M.; Friedrich, B. Synthesis of Titanium-Based Powders from Titanium Oxy-Sulfate Using Ultrasonic Spray Pyrolysis. *Materials* **2024**, *17*, 4779. [[CrossRef](#)]
23. Das, R.; Pachfule, P.; Banerjee, R.; Poddar, P. Metal and metal oxide nanoparticle synthesis from metal organic frameworks (MOFs): Finding the border of metal and metal oxides. *Nanoscale* **2012**, *4*, 591–599. [[CrossRef](#)]
24. Bang, H.; Suslick, K. Application of Ultrasound to the Synthesis of nanostructured Materials. *Adv. Mater.* **2010**, *22*, 1039–1059. [[CrossRef](#)] [[PubMed](#)]
25. Perendis, D. Thin Film Deposition by Spray Pyrolysis and the Application in Solid Oxide Fuel Cells. Ph.D. Thesis, ETH Zurich, Zürich, Switzerland, 2003.
26. Jokanović, V.; Janačković, D.; Spasić, A.; Uskoković, D. Synthesis and formation mechanism of ultrafine spherical Al₂O₃ powders by ultrasonic spray pyrolysis method, *Materials Transactions. JIM* **1996**, *37*, 627–635.
27. Tang, W.; Khavarian, M.; Yousefi, A. Red Mud. In *Sustainable Concrete Made with Ashes and Dust from Different Sources: Materials, Properties and Applications*; Woodhead Publishing: Sawston, UK, 2022; pp. 577–606.
28. Verma, A.S.; Suri, N.M.; Kant, S. Applications of Bauxite Residue: A Mini-Review. *Waste Manag. Res.* **2017**, *35*, 999–1012. [[CrossRef](#)]
29. Sutar, H.; Mishra, S.C.; Sahoo, S.K.; Chakraverty, A.P.; Maharana, H.S. Progress of Red Mud Utilization: An Overview. *Chem. Sci. Int. J.* **2014**, *4*, 255–279. [[CrossRef](#)]
30. Morsali, S.; Yildirim, F. Environmental Impact Assessment of Red Mud Utilization in Concrete Production: A Life Cycle Assessment Study. *Environ. Dev. Sustain.* **2024**, *26*, 12219–12238. [[CrossRef](#)]

Disclaimer/Publisher’s Note: The statements, opinions and data contained in all publications are solely those of the individual author(s) and contributor(s) and not of MDPI and/or the editor(s). MDPI and/or the editor(s) disclaim responsibility for any injury to people or property resulting from any ideas, methods, instructions or products referred to in the content.